Landscape Ecol
DOI 10.1007/s10980-013-9908-7

RESEARCH ARTICLE

Assessing the effects of subtropical forest fragmentation on leaf nitrogen distribution using remote sensing data

Moses Azong Cho · Abel Ramoelo · Pravesh Debba · Onisimo Mutanga · Renaud Mathieu · Heidi van Deventer · Nomzamo Ndlovu

Received: 28 January 2013 / Accepted: 5 June 2013

Abstract Subtropical forest loss resulting from conversion of forest to other land-cover types such as grassland, secondary forest, subsistence crop farms and small forest patches affects leaf nitrogen (N) stocks in the landscape. This study explores the utility of new remote sensing tools to model the spatial distribution of leaf N concentration in a forested landscape undergoing deforestation in KwaZulu-Natal, South Africa. Leaf N was mapped using models developed from RapidEye imagery; a relatively new space-borne multispectral sensor. RapidEye consists of five spectral bands in the visible to near infra-red (NIR) and has a spatial resolution of 5 m. MERIS terrestrial chlorophyll index derived from the RapidEye explained 50 % of the variance in leaf N across different land-cover types with a model standard error of prediction of 29 % (i.e. of the observed mean leaf N) when assessed on an independent test data. The results showed that indigenous forest fragmentation leads to significant losses in leaf N as most of the land-cover types (e.g. grasslands and subsistence farmlands) resulting from forest degradation showed lower leaf N when compared to the original indigenous forest. Further analysis of the spatial variation of leaf N revealed an autocorrelation distance of about 50 m for leaf N in the fragmented landscape, a scale corresponding to the average dimension of subsistence fields (2,781 m^2) in the region. The availability of new multispectral sensors such as RapidEye thus, moves remote sensing closer to widespread monitoring of the effect of tropical forest degradation on leaf N distribution.

Keywords Subtropical forest fragmentation · Leaf nitrogen · Remote sensing

M. A. Cho (✉) · A. Ramoelo · R. Mathieu · H. van Deventer
Earth Observation Group, Natural Resources and Environment (NRE), Council for Scientific and Industrial Research (CSIR), P.O. Box 395, Pretoria 0001, South Africa
e-mail: mcho@csir.co.za

P. Debba
Built Environment, Council for Scientific and Industrial Research (CSIR), Pretoria, South Africa

O. Mutanga
School of Agricultural, Earth & Environmental Sciences, University of KwaZulu-Natal, P. Bag X01, Scottsville, Pietermaritzburg 3209, South Africa

N. Ndlovu
Department of Agriculture, Forestry and Fisheries (DAFF), Pretoria, South Africa

Introduction

Tropical forest ecosystems play a major role in nutrient and carbon cycling (Vitousek and Sanford 1986; Van der Werf et al. 2009). For example, tropical forests constitute a major sink of atmospheric carbon dioxide and several studies have shown that tropical

Published online: 19 June 2013

forest deforestation and degradation were major sources of global greenhouse emission in the 1990s (Malhi and Grace 2000; Achard et al. 2004; Fearnside and Laurance 2004; Gibbs et al. 2007; DeFries et al. 2002). Gibbs et al. (2007) put the estimates at about 15–25 % of annual global greenhouse gas emissions. Whereas, the effects of forest disturbance on carbon stocks at the broad landscape level have been widely studied, few studies have modelled the effects of forest degradation on nutrient stocks (e.g. Nitrogen (N) and phosphorus (P)) (e.g. Billings and Gaydess 2008).

Tropical forest degradation in many parts of Africa is characterised by the clearing of the forest for pasture, agriculture or urban development (Van Wyk et al. 1996; Coops et al. 2004). In most cases, the forest is fragmented into patches of various sizes and shapes surrounded by a matrix of different vegetation and/or land-use types (e.g. mono-crop plantations, small subsistence farms, pasture lands) (Saunders et al. 1991; Herrera et al. 2011). The immediate environmental consequences of forest fragmentation include soil erosion, loss of biodiversity, invasion by alien species, loss of soil fertility, changes in litter and canopy nutrient stocks and vegetation productivity (Saunders et al. 1991; Gibbs 1998; McDonald et al. 2002; Vasconcelos and Luizão 2004; Giertz et al. 2005; Lauga and Joachim 1992; Duguay et al. 2007; Lizée et al. 2012). Spatially explicit information on the above factors is rare, let alone on changes in foliar nutrient stocks, following forest fragmentation. Saunders et al. (1991) asserted that forest fragmentation affects nutrient cycling processes by increased soil heating and associated effect on soil microorganism and invertebrate numbers and activity, on litter decomposition and soil moisture retention. The resulting loss of soil fertility might translate into low foliar nutrient stocks.

Nitrogen is an important nutrient for plant growth (Groffman and Turner 1995). Nitrogen taken up by plants in the form of nitrates is used in the synthesis of components such as chlorophyll, the carbon fixing enzyme ribulose biphosphate carboxylase (Rubisco) and inert structural components in cell tissue (Mooney 1986). Hence leaf N concentration has been used as a proxy to assess ecosystem productivity (Mooney 1986; Smith et al. 2002). Nitrogen inputs into an ecosystem include lightning and bacteria fixation of atmospheric N, and decomposition and nitrification of dead organic matter (e.g. litter). Outputs from the system include plant uptake, denitrification, leaching and surface runoff. Thus, forest N pools consist of soil N (ammonium, nitrate, and some dissolved organic N compounds), N in litter and in living plant parts (roots, stems and leaves) (Vitousek 1982). Rates of organic matter decomposition are higher in lowland moist tropical forest than in temperate forest (Nye 1960). Greenland and Kowal (1960) argued that standing biomass is as important as the soil as a storehouse of plant nutrients, particularly in moist tropical forest where vegetation growth is so high and where the reserves of nutrients in the soil may be quite rapidly depleted by leaching or absorbed by plants. Vitousek and Sanford (1986) asserted that foliar chemistry represents a useful indicator of overall nutrient status of a plant, where nutrient concentrations in leaves are correlated with nutrient concentrations in other plant parts. Leaching and surface runoff of nutrients from moist tropical forest patches in a degraded landscape might serve as important nutrient sources for surrounding vegetation, including grasslands and subsistence farms.

The question is, how does the conversion of indigenous tropical forest into other land-cover types e.g. grassland, secondary forest, subsistence crop farms and small forest patches affect foliage N stock in the fragmented landscape? Another question of interest is, at what scale does leaf N vary in fragmented or disturbed landscape. The ability to adequately tackle the above questions may rely on our capability to accurately map land-cover types and leaf N concentration at the broad landscape level, a procedure that was rarely achieved before the advent of high spectral resolution (hyperspectral) remote sensing (Iverson et al. 1989; Groom et al. 2006). Most hyperspectral sensors acquire radiance information in less than 10 nm bandwidths from the visible to the shortwave infrared (400–2,500 nm) (Curran 2001). The narrow bandwidth of hyperspectral data allows for the detection of the subtle absorption features of N in green vegetation (Curran et al. 2001; Cho et al. 2010a). However, the high cost and limited availability of space-borne hyperspectral imagery has stymied the routine application of this sort of remote sensing for leaf N analysis at the regional scale. Many hyperspectral studies highlighted the region of the red-edge in the electromagnetic spectrum (700–760 nm) as having a high potential for accurate estimation of leaf chlorophyll and N at peak productivity (Horler et al.

1983; Matson et al. 1994; Kokaly and Clark 1999; Cho and Skidmore 2006). More recently, new space-borne sensors such as RapidEye and WorldView-2 have been launched with new wavebands in the red-edge region, for example at 710 nm for Rapideye and at 725 nm for WorldView-2. These sensors provide us with new opportunities to assess leaf N stock and other vegetation variables at the regional scale e.g. mapping leaf N using RapidEye (Ramoelo et al. 2012), papyrus biomass using WorldView-2 imagery (Mutanga et al. 2012), rangeland N concentration (Zengeya et al. 2013) and forest structural parameters (Ozdemir and Karnieli 2011).

The aims of this study were to (i) ascertain the ability to assess leaf N concentration using RapidEye imagery in a fragmented landscape following indigenous forest degradation and (ii) assess the effects of forest fragmentation on leaf N distribution at the broad landscape. The study therefore goes beyond assessing the utility of RapidEye imagery for mapping leaf N for grasslands only as already demonstrated by Ramoelo et al. (2012) to assessing leaf N in a heterogeneous landscape consisting of closed subtropical forests, grasslands and cultivated areas. The spatial variability of nitrogen in subtropical forest area following deforestation has rarely been studied. The aims were achieved through a detailed land-cover classification using WorldView-2 images, mapping of leaf N using RapidEye images, an analysis of the differences in the predicted leaf N among land-cover types and an analysis of the spatial heterogeneity of leaf N.

Materials and methods

Study site

The study site is situated in the northern part of KwaZulu-Natal, South Africa between Mtubatuba town and the Indian Ocean, north of Richard's Bay (Fig. 1). It consists of three main ecosystem types; intact closed canopy forest (inland coastal forest and dune forest), swamp forest and fragmented landscape. The inland coastal forest is known as the Dukuduku forest (28°25′S, 32°17′E). The Dukuduku forest is the largest patch (6,500 ha) of coastal lowland forest along the eastern coastline in KwaZulu-Natal. A total of 29 % of the Dukuduku forest was lost to settlement and subsistence farming activities between 1992 and 2005 (Ndlovu et al. 2011). The area forms part of the iSimangaliso Wetland Park which is the largest estuary in South Africa (Van Heerden 2011). The study area as demarcated by the map in Fig. 1 is surrounded by large commercial *Eucalyptus* (to the North) and Sugarcane (to the South) plantations. Thus, the study area consists of varying land uses including protected areas, commercial farms, communal areas and towns.

Acquisition of satellite images and pre-processing

RapidEye imagery (5 m spatial resolution) was acquired on 21 March 2011. The sensor consists of five spectral bands centred at 475 nm (blue), 555 nm (green), 657.5 nm (red), 710 nm (red-edge) and 805 nm (NIR). The level 1B RapidEye image (geometrically and radiometrically corrected) obtained from the image provider were atmospherically corrected using ATCOR-2, flat terrain model. ATCOR is based on MODTRAN radiative transfer code (Richter and Schlapfer 2002). Two archive geometrically corrected WorldView-2 images (2 m spatial resolution) acquired in April and December of 2010 were also used in the study to classify land-cover types. Worldview-2 consists of eight multispectral bands centred at 425 nm (coastal), 480 nm (blue), 545 nm (green), 605 nm (yellow), 660 nm (red), 725 nm (red-edge), 835 nm (NIR1) and 950 nm (NIR2). We assessed the geometric accuracies of the two images using ground control GPS points and found the WorldView-2 images more accurately corrected as compared to the RapidEye image. Using the WorldView-2 as the reference image, we re-projected the RapidEye image using image–image registration in ENVI software (ITT Visual Information Solution, Boulder Co USA). In this study, the WorldView-2 images were used for the land-cover classification because of the better spatial resolution when compared to RapidEye. WorldView-2 could not be used for assessing leaf N because of large time difference between the image acquisition (April and December 2010) and the field campaign to collect leaf N data (March 2011).

Field data acquisition and leaf nitrogen analysis

Field sampling of leaf specimens was conducted on the 29 and 30 March 2011. Sunlit leaves were

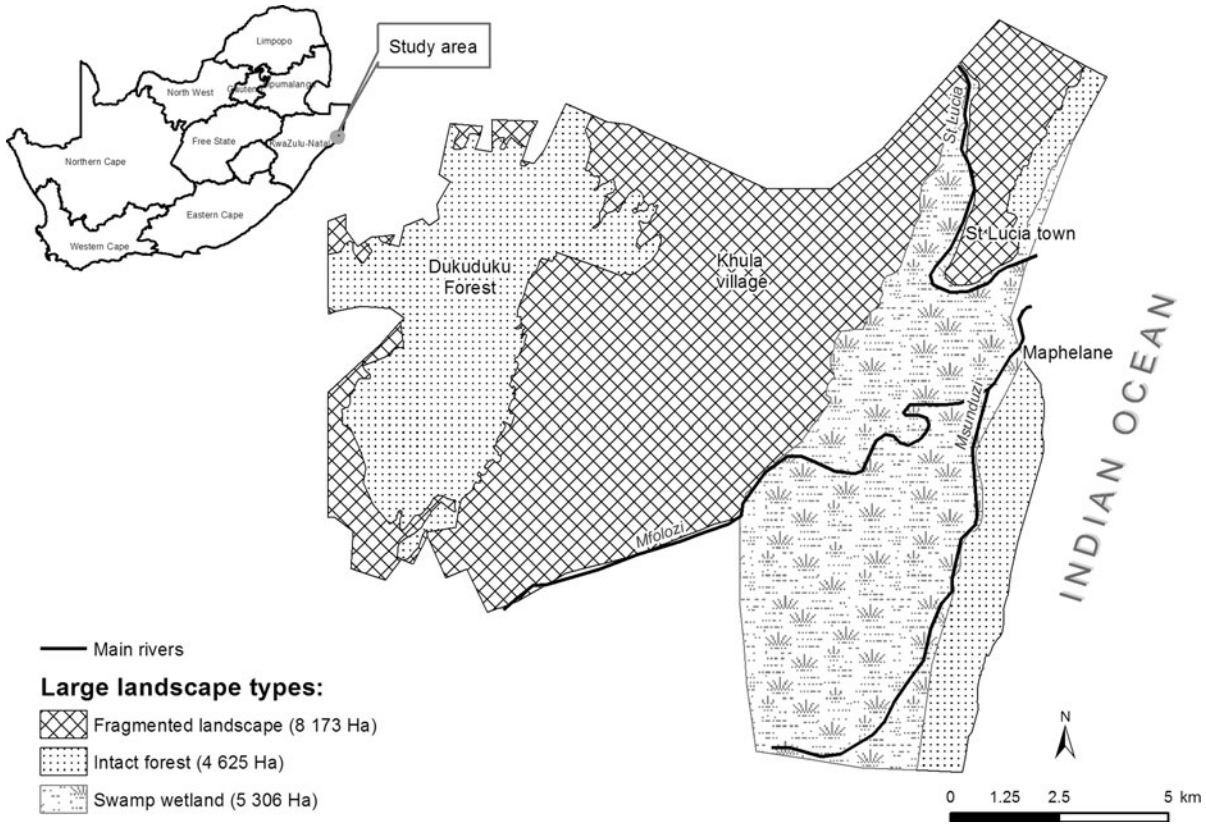

Fig. 1 Large landscape types

collected from 69 randomly selected plots consisting of tree or grass canopies along foot paths in the intact and fragmented landscape. We ensured that each tree or grass canopy sampled consisted of a homogenous canopy (same species for the trees and similar set of species for the grasses) of about 15 m by 15 m. The sampled trees and grass plots were located between 10 m to about 100 m from the edges of intact forest and paths within the fragmented landscape. 44 and 25 of the plots were tree canopies and grassland areas, respectively. Five and two plots of the grassland plots were wetlands and sugarcane farms, respectively.

The leaf specimens were oven dried for 24 h at 70 °C on the 31 April 2011. The dry leaf samples were sent to the Agricultural Research Council-Institute for Tropical and Subtropical Crops, South Africa for chemical analysis of leaf N. Leaf N concentration was analysed using acid digestion method (Novozamsky et al. 1983). Leaf N concentration was expressed as the percentage N to the leaf mass.

Additional data were collected for the land cover classification in July 2011. Randomly selected GPS locations of different land cover (LC) types (intact forest, degraded forest, grassland/subsistence farms, *Eucalyptus* farms, sugarcane farms) were recorded in the field. The points were only collected from homogenous areas (of at least 20 m by 20 m) of the land-cover types.

Land-cover (LC) classification

The WorldView-2 images were used for the LC classification. A mosaic of the April and December 2010 images was made prior to the classification. The classification was conducted using ENVI 4.8 software (ITT Visual Information Solution, Boulder Co USA). The GPS positional data for the various land cover types (intact forest, degraded forest, grassland/subsistence farms, *Eucalyptus* farms, wetland grasslands and sugarcane farms) were overlaid on the image and a region of interest (ROI) consisting of an array of pixels was created for each point. Additional ROIs were created for the intact forest and wetland grasslands (mainly from the swamp forest) since these were

clearly visible on the WorldView-2 image. The ROIs were randomly divided into the training and test datasets in the following ratio: intact natural forest (44/17), grassland/subsistence farms (11/6), wetland grasslands (47/21), degraded forest (25/10), *Eucalyptus* farms (18/13), sugarcane farms (24/8), bare soil and settlements (22/11). The commonly used maximum likelihood classifier was used in this study because it accounts for within-class first order (mean) and second order (variance) variations (Cho et al. 2010b) The classification accuracy was assessed using commonly used measures such as the overall, producer's and user's accuracies. These measures are usually computed from the confusion or error matrix constructed with the mapped cover types represented as rows and the reference ('ground-truthing') data as columns. The overall accuracy is then derived as the proportion of the area mapped correctly, the user's accuracy as the proportion of area mapped as a particular class that is actually that class in the field and the producer accuracy as the proportion of the areas that is a particular class in the field that is also mapped as that class (Skidmore 1999). The area is often calculated as a product of the number of pixels and the pixel size. However, Conese and Maselli (1992), Olofsson et al. (2013) argued that the pixel counting approach described above is biased for the true population of area in the presence of asymmetric classification errors. We therefore, computed the error matrix in terms of the unbiased estimators of the proportion of the area in each cell of the error matrix as proposed by Olofsson et al. (2013). Subsequently, the unbiased estimator of the total area (including the 95 % confidence interval) of each class was computed from the estimated error matrix.

Regression analysis and mapping of leaf nitrogen

The GPS points of the field sample plots were overlaid on the atmospherically corrected RapidEye images and the tree or grass canopy spectral profiles were extracted using an array of 2-by-2 pixels. Several red-edge spectral indices that have shown great promise for leaf N or chlorophyll estimation in previous studies including Gitelson and Merzlyak index (Gitelson and Merzlyak 1997), Datt index (Datt 1998, 1999) and the MERIS terrestrial chlorophyll index (MTCI) (Dash and Curran 2007) were computed from the spectral profile. The classical normalised difference vegetation index (NDVI) (Rouse et al. 1974) was also calculated for comparison with the red-edge spectral indices. After exploring the relationship between leaf N and the red-edge indices, the MTCI was chosen for the prediction of leaf N in the study area as it provided the highest linear regression coefficient of determination (R^2).

It should be noted that the MTCI was originally derived for leaf chlorophyll estimation. We have used this index to estimate leaf N because leaf chlorophyll is a good correlate of leaf N, particularly at peak productivity (Yoder and Pettigrew-Crosby 1995). The strength of the linear relationship between leaf N and the MTCI was assessed using a bootstrapped (McGarigal et al. 2000) linear regression because of the small number of sample points. The regression coefficients were computed for 1,000 iterative sampling with replacement, i.e. for each iteration, 2/3 of the data were randomly drawn and used for calibration of the regression model and the remaining 1/3 for validation. For each iteration, the root-mean-square error (RMSE) of calibration and validation (termed standard error of prediction (SEP)) were computed. An MTCI map was derived from the RapidEye image using the ENVI 4.8 Band Math feature. Using the linear regression equation involving MTCI and leaf N derived from the bootstrapped process, a leaf N concentration map was then computed from the MTCI map. The slope and intercept of the regression line were the average values for the 1,000 bootstrapped iterations.

To evaluate the effect of forest fragmentation on leaf N stock, the land-cover map derived from the WorldView-2 imagery was spatially re-sampled to a spatial resolution of RapidEye i.e. to 5 m. Differences in leaf N concentration between the different land-cover classes were assessed. First, ROIs for the different land cover classes were created and overlaid on the leaf N Map. Subsequently, leaf N values for the different land cover classes were extracted from the N map and tables for the leaf N values were then created. The differences among the various land cover classes were assessed using descriptive statistics including a table of mean and inter-quartile ranges, and box plots.

Characterising spatial heterogeneity of leaf nitrogen concentration

The spatial variation or heterogeneity of leaf N in the intact and fragmented regions was analysed using

semivariogram models (Garrigues et al. 2006; Murwira and Skidmore 2006). Semivariogram modelling involves the hypothesis of statistical stationarity i.e. the characteristics of the underlying random function are invariant to the shifting of a group of pixels from one part of the image to another (Garrigues et al. 2006). In this study, we assessed the spatial variation of leaf N from exponential models fitted to experimental semivariograms (Eq. 1). The exponential model was adopted in this study as it provided the best fit when compared to the spherical and Gaussian models.

$$\gamma(h) = \frac{1}{2n}\sum_{n(h)}[z(u) - z(u+h)]^2 \quad (1)$$

where $\gamma(h)$ are the semivariances, $z(u)$ is the pixel value at position u in the input map, $z(u + h)$ is the pixel value at position $u + h$ in the input map and h is the lag vector representing separation (distance) between two spatial points (pixels). We used a lag tolerance of 200 pixels (1,000 m). Two parameters that describe a semivariogram are of particular importance in this study: (i) the sill represents the point (semivariance) at which a semivariogram levels off and (ii) the range represents the lag distance at which a semivariogram reaches the sill. The range describes the size or scale of the dominant objects in an image that give rise to the semivariogram structure (Jupp et al. 1988). The semivariograms were modelled using the Integrated Land and Water Information System (ILWIS) software (ITC, Enchede, The Netherlands).

Results

Land-cover classification from WorldView-2 imagery

An overall classification accuracy of 88 % (computed from the error matrix of estimated area proportions) was obtained for the land-cover classification (Fig. 2; Table 1). With the exception of the normal grassland class (pasture and farmlands), the producer's and user's accuracies were in general high (Table 1). The low user's accuracy (44 %) for the grassland class was due to a miss-classification of wetland grassland pixels (16 % of wetland pixels) into other grasslands (pasture and farmlands). Natural forest remains by far the largest (7,126 ha) land-cover type in the study area followed by wetland grasslands (Table 2). The average patch size of natural forest, *Eucalyptus* farms, grasslands (pasture and subsistence farms) and sugarcane farms in the fragmented landscape are 5,900 m^2 (0.59 ha), 3,100 m^2 (0.31 ha), 1,500 m^2 (0.15 ha) and 625 m^2 (0.0625 ha), respectively; yielding an overall patch size of 2,781 m^2 (0.2781 ha).

Statistics of laboratory measured leaf nitrogen

The laboratory measured leaf N showed the following statistics; average = 2.19 %, maximum = 4.76 %, minimum = 0.70 % and standard deviation (SD) = 0.94 %. The grass leaf N concentration (mean = 1.38 %) was significantly (p value < 0.0001) lower than the tree leaf N (mean = 2.66 %) (Fig. 3). Furthermore, a Shapiro–Wilk normality test conducted on the data showed that the leaf N data for grasses and trees were normally distributed; grass ($W = 0.92$, p value > 0.05) and trees ($W = 0.98$, p value > 0.05).

Mapping leaf nitrogen from RapidEye imagery

Amongst the four vegetation indices investigated, the MTCI yielded the highest linear regression coefficient of determination with leaf N (mean $R^2 = 0.52$, SD = 0.05) and the lowest prediction error on the test data (SEP = 0.65 % i.e. 29 % of mean leaf N, SD = 0.08) (Table 3; Fig. 4). The commonly used NDVI yielded the highest prediction error (SEP = 0.77, SD = 0.1) amongst the indices applied in the study. The regression model based on the MTCI (Eq. 2) was used to predict leaf N concentration for every pixel on the RapidEye image (Fig. 5).

$$[N] = 0.8926 * MTCI - 0.6103 \quad (2)$$

where [N] is the leaf N concentration (%). The slope of the line of best fit (0.8926) and the intercept (−0.6103) were the means for 1,000 bootstrapped iterations.

Differences in predicted leaf nitrogen among land cover types

Table 4 shows the descriptive statistics of predicted leaf N for the large intact forest areas (intact inland coastal forest and dune forest) and leaf N of land-cover types in the degraded landscape including small natural forest patches, degraded forest patches, grasslands, *Eucalyptus* and sugarcane farms. Among the

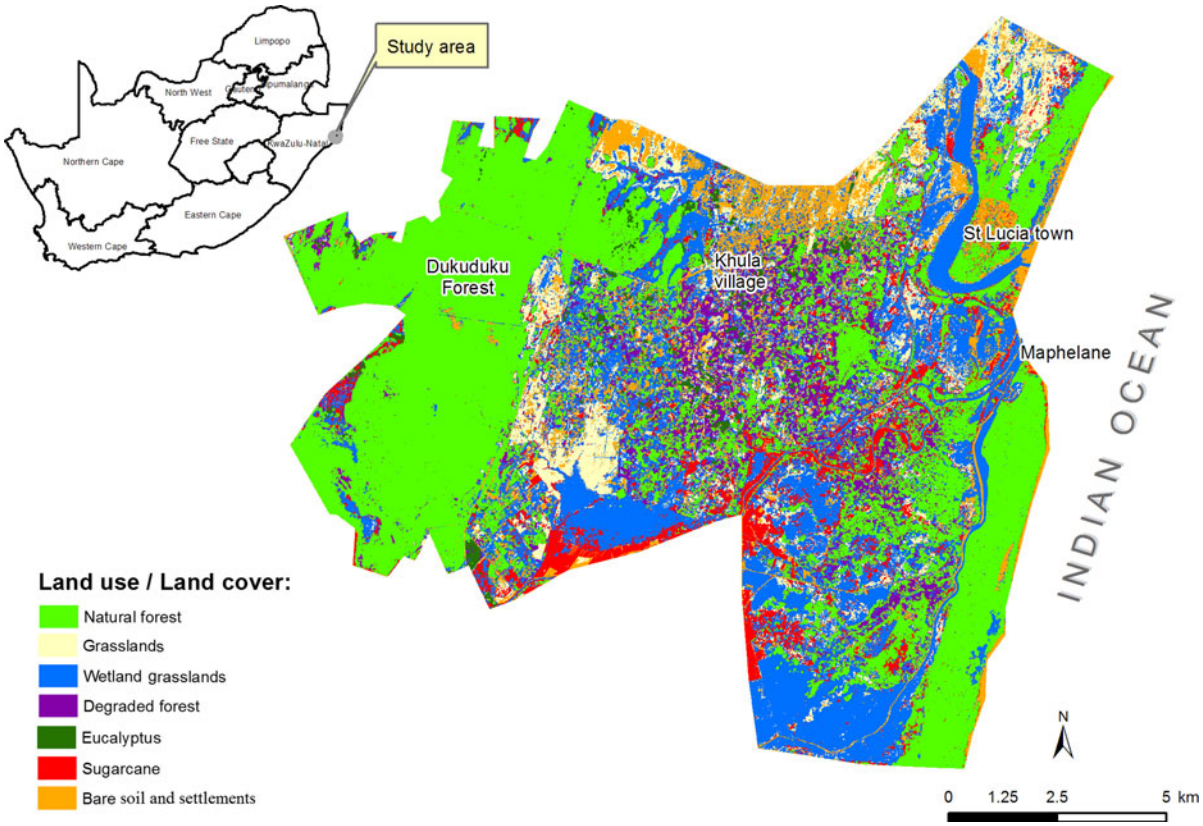

Fig. 2 Land cover classes for the study area derived from WorldView-2

Table 1 Classification accuracies for land-cover types in the study area using WorldView-2 imagery

Land-cover type	Producer's accuracy (%)	User's accuracy (%)
Natural forest (the intact forest and patches in the fragmented landscape)	96	94
Grasslands (pasture and farmlands)	76	44
Wetland grasslands	79	97
Degraded forest (thickets of shrubs, secondary forest trees and invasive aliens)	88	90
Eucalyptus farms	94	89
Sugarcane farms	95	67
Bare soil and settlements	78	99

cover types, *Eucalyptus* farms showed the highest average leaf N concentration (mean = 3.13 %). The conversion of intact forest into grasslands significantly reduces the leaf N stock in the landscape; from mean N of 2.93–1.45 % (a 50 % decrease). The natural forest fragments in the disturbed area showed leaf N concentrations (mean = 2.47 %) slightly less than (by 16 %) values for the large intact forest areas (mean = 2.93 %). While a 22 % decreased in leaf N from the intact to the degraded forest was observed.

Scale of leaf nitrogen variability

Leaf N showed a higher autocorrelation distance (range = 50 m) in the fragmented landscape when compared to the intact forest (range = 25 m) (Table 5; Fig. 6). Furthermore, the semi-variogram of the intact forest showed a lower sill (0.26) when compared to the sill (0.5) of the fragmented landscape.

Discussion

This study ascertains the utility of RapidEye imagery for mapping leaf N concentration at the broad

landscape scale, though with a relatively modest R^2 (0.5). Using RapidEye imagery, Ramoelo et al. (2012) obtained a lower R^2 (0.23) but for estimating leaf N concentration for only savannah grasslands which exhibit a lower range of leaf N variation than trees. The above regression R^2 are lower compared to those reported with hyperspectral remote sensing e.g. Mutanga et al. (2004) obtained $R^2 = 0.7$ for savannah grassland using field spectroscopy or $R^2 = 0.78$ in Boegh et al. (2002) for an agricultural area using airborne hyperspectral images. However, the improvements shown by RapidEye over conventional multispectral sensor such as Landsat is a significant step forward in mapping of leaf N concentration at the broad landscape scale. The improved results from RapidEye imagery can be attributed to the presence of the red-edge band at 710 nm. MTCI, an index derived from the red-edge band at 710 nm provided a higher accuracy of estimation of leaf N in this study when compared to the traditional NDVI derived from reflectance at 805 and 660 nm. Variations in the red-

Table 2 Surface area of land-cover classes in the study area based on the classification

Land cover class (LC)	Total area (ha)	±95 % CI
Natural forest	7,126	107
Grassland/subsistence farms	999	38
Wetland grasslands	5,706	94
Degraded forest	1,423	100
Eucalyptus farms	310	54
Sugarcane farms	957	64
Bare soil and settlements	1,575	30
Total area (ha)	18,097	

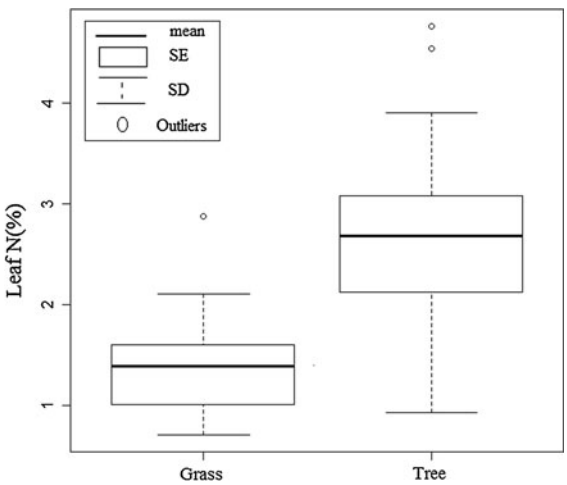

Fig. 3 Laboratory measured leaf N for grasses and trees

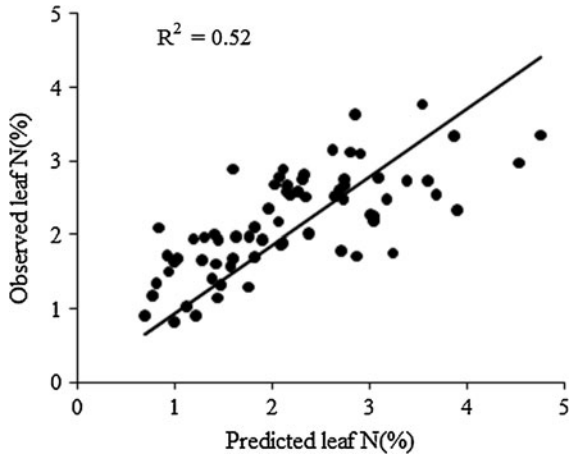

Fig. 4 Linear relationship between observed and predicted leaf N concentration using linear regression models for MERIS terrestrial chlorophyll index (MTCI)

Table 3 Training and validation results for predicting leaf nitrogen concentration based on bootstrapped linear regression for 1,000 iterations

Index	Formulation (R_λ = reflectance at wavelength centre (λ nm))	Calibration model				Validation	
		Av R^2	SD R^2	Av RMSE	SD RMSE	Av SEP	SD SEP
NDVI	$(R_{805} - R_{657})/(R_{805} + R_{657})$	0.34	0.05	0.75	0.05	0.77	0.10
Datt	$(R_{805} - R_{710})/(R_{805} - R_{657})$	0.49	0.04	0.66	0.04	0.68	0.08
SR	R_{805}/R_{710}	0.47	0.05	0.67	0.04	0.70	0.08
MTCI	$(R_{805} - R_{710})/(R_{710} - R_{657})$	0.52	0.05	0.64	0.04	0.66	0.08

R^2 coefficient of determination, *RMSE* root mean square error for the calibration model, *SEP* standard error of prediction, *Av* average, *SD* standard deviation, *NDVI* normalised difference vegetation index, *Datt index* named after Datt (1998), *SR* simple ratio (Gitelson and Merzlyak 1997), *MTCI* MERIS terrestrial chlorophyll index

edge reflectance are mostly controlled by differences in leaf chlorophyll concentration (Horler et al. 1983). Therefore, the positive correlation between leaf N and MTCI depends on the positive correlation relationship between leaf N and leaf chlorophyll (Yoder and Pettigrew-Crosby 1995; Huang et al. 2004). Most of the spectral absorption features of N are located in the shortwave infrared (SWIR) e.g. at 2,190 nm (Curran 1989). Therefore, new multispectral space-borne sensors with strategic bands in the SWIR such as the upcoming space-borne Sentinel-2 sensor of European Space Agency (ESA) might provide new opportunities to routinely assess leaf N.

The effect of forest fragmentation in leaf N was assessed using a detailed classified map of land-cover types produced WorldView-2. Generally high producers' and users' accuracies were obtained from the classification with the exception of the grasslands class where there was a high confusion with the wetland grassland class. Although the effect of the mosaicking of two WorldView-2 images acquired on two different dates on the classifier was not explicitly studied, there was no visual evidence of the effect of radiometric discrepancies on the classified map.

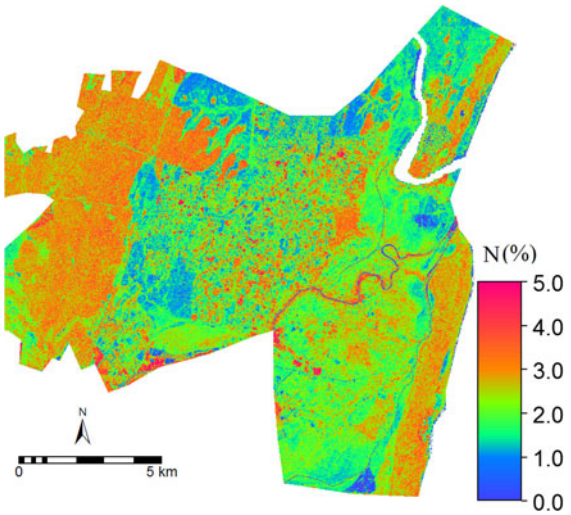

Fig. 5 Leaf N concentration (%) in the study area

The results of this study show that deforestation and the subsequent conversion of the degraded area into grasslands leads to loss of foliar N from the system. The results show a decreasing gradient of leaf N from the intact forest, forest patches in the fragmented landscape, degraded forest patches to the grasslands areas. The cleared areas in the study site are mostly used for farming of crops such as sweet potato, maize and sugarcane, and for grazing. The sandy soils in the area are low in fertility. Thus, soil fertility in the area is highly dependent on the decomposition of the dead organic matter, reason for which crop production declines quickly after 1–2 years of farming on the cleared land. Furthermore, farming methods used in this area (mostly slash and burn) are not adequate to maintain soil fertility for long periods of time. Farmers often resort to clearing more forest area to acquire new fertile lands. The vicious cycle of forest clearance and poor farming methods leads to soil depletion fertility and subsequent clearing of new fertile forest land, resulting in a high rate of forest loss and therefore loss of N from the system. However, patches of indigenous forest within the degraded areas still retain relatively high concentration of N in their foliage. This also applies to *Eucalyptus* trees which are exotic species

Table 5 Exponential model parameters for semi-variograms of leaf nitrogen for the intact indigenous forest and fragmented landscape

Land cover type	Nugget	Sill	Range (m)
Intact indigenous forest	0.05	0.26	25
Fragmented landscape	0.05	0.5	50

Table 4 Statistics of predicted leaf nitrogen (%) per land-cover class

	Intact inland forest	Dune forest	Natural forest in fragmented landscape	Degraded forest in fragmented landscape	Grasslands/subsistence in fragmented landscape	*Eucalyptus*	Sugarcane
Mean	2.93	2.77	2.47	2.27	1.45	3.13	2.03
1st quartile	2.59	2.48	1.950	1.82	1.26	2.44	1.53
3rd quartile	3.27	3.09	2.98	2.68	1.56	3.80	2.40
SD	0.52	0.55	0.70	0.61	0.31	0.96	0.69

SD standard deviation

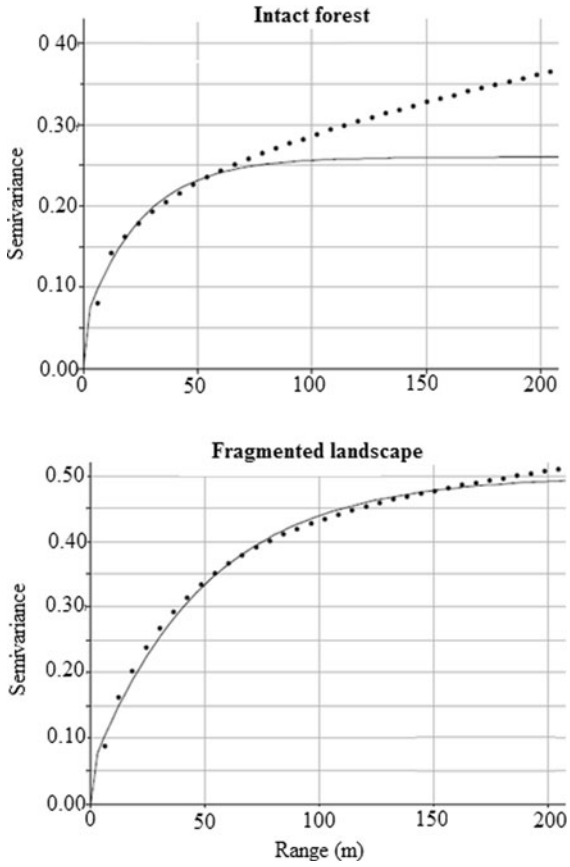

Fig. 6 Semivariograms of leaf nitrogen for the intact forest and fragmented landscape

grown in the degraded area. We do not know whether the high N in *Eucalyptus* leaves is due to artificial N fertilisation of *Eucalyptus* farms or this species ability to assimilate high N in its leaves.

The loss of N stock following forest degradation in the tropics is a well-known phenomenon (Piccolo et al. 1994; Davidson et al. 2004). However, the ability to map leaf N at the broad landscape facilitates the task of analysing the effect of forest degradation on the spatial distribution of leaf N on a plot-by-plot level, thus permitting a better understanding of different landscape patterns and processes. Mapping leaf N at the scale of the RapidEye images (5 m) in the tropical forest systems of Africa would allow for a farm-to-farm assessment of leaf N stocks because of the usual small sizes of subsistence fields. For example, the lower autocorrelation distance of leaf N variability in the intact forest (25 m) when compared to the fragmented landscape (50 m) probably corresponds to tree crown level variability while the autocorrelation distance in the fragmented landscape might depict spatial dependence at the scale of subsistence fields (e.g. crop and *Eucalyptus* farms) in the region (i.e. 2,500 m^2 for a rectangular field). Indeed the land-cover classification yielded an average patch size of 2,781 m^2 in the fragmented landscape. The semivariogram sill is higher in the fragmented landscape depicting more variability of leaf N at the 50 m scale when compared to the variability of leaf N at the autocorrelation scale of 25 m in the intact forest. This indicates more variability of leaf N within the subsistence farms. Many subsistence farms consist of a mixture of different crops, thus creating a high variability of leaf N. We conclude that the ability to map leaf N at the farm-size scale might provide a greater understanding of the different land management or farming practices at that scale. This is even more relevant in the tropical forest region of Africa, where more than 80 % of the population depends on subsistence farming for their livelihoods.

The results of this study could have some management implications. The patches of forest in the degraded area which still showed high leaf N when compared to grasslands can serve as nutrient sources for the surrounding farmlands, i.e. leaching and surface runoff from the forest patches might feed adjacent grasslands and farmlands with nutrients. Further research will be needed to ascertain the roles of both indigenous trees and exotic *Eucalyptus* farms as nutrient sources to surrounding grasslands and farmlands in the study area. However, the benefits of domestication of indigenous tree species over subsistence commercial *Eucalyptus* plantations have been highlighted in the past two decades (Leakey and Simons 1998; Simons and Leakey 2004). Although the commercial value of domesticated indigenous trees might not meet those of *Eucalyptus* in the study area e.g. for the construction business, agroforestry and non-timber products of domesticated indigenous species offer a number of benefits to the poor rural communities in comparison to commercial plantation, which may include:

- Indigenous forests provide food resources, raw material for craft work and medicine to the poor rural communities
- Indigenous species might sustain more diversity of plants and animals in the area when compared to the subsistence *Eucalyptus* farms

- Patches of indigenous trees may provide corridors of faunal and floral dispersion

Prasad (2003) has recommended that mixed farming practices with patches of indigenous tree species should be encouraged in fragmented landscapes to help sustain biodiversity in degraded tropical forest. On the other hand, allelochemicals in *Eucalyptus* leaf litter may suppress growth of understorey vegetation (May and Ash 1990).

Conclusions

The following conclusions could be drawn from the study:

- The MERIS Terrestrial Chlorophyll Index (MTCI) derived from RapidEye imagery explained 52 % of leaf N variability in the study area consisting of various land-cover types (natural forest, grasslands, wetland grasslands, *Eucalyptus* and sugarcane farms), thus ascertaining the utility of RapidEye sensor for mapping leaf N.
- Indigenous forest fragmentation significantly affects the distribution of leaf nitrogen concentration in the landscape.

Acknowledgments The Council for Scientific and Industrial Research (CSIR) and the Department of Science and Technology (DST) provided the funding for this study. We wish to thank Oupa Malahlela for atmospherically correcting the RapidEye images used in the study. We also express gratitude to Mr. Khanyile MM, the manager of the Dukuduku forest for his wonderful cooperation throughout the project.

References

Achard F, Eva HD, Mayaux P, Stibig HJ, Belward A (2004) Improved estimates of net carbon emissions from land cover change in the tropics for the 1990s. Glob Biogeochem Cycles 18:GB2008

Billings S, Gaydess E (2008) Soil nitrogen and carbon dynamics in a fragmented landscape experiencing forest succession. Landscape Ecol 23:581–593

Boegh E, Soegaard H, Broge N, Hasager CB, Jensen NO, Schelde K, Thomsen A (2002) Airborne multispectral data for quantifying leaf area index, nitrogen concentration, and photosynthetic efficiency in agriculture. Remote Sens Environ 81:179–193

Cho MA, Skidmore AK (2006) A new technique for extracting the red edge position from hyperspectral data: the linear extrapolation method. Remote Sens Environ 101:181–193

Cho MA, van Aardt J, Main R, Majeke B (2010a) Evaluation of variations of physiology-based hyperspectral features along a soil water gradient in *Eucalyptus grandis* plantation. Int J Remote Sens 31(12):3143–3159

Cho MA, Debba P, Mathieu R, Naidoo L, Van Aardt J, Asner GP (2010b) Improving discrimination of savanna tree species through a multiple-endmember spectral angle mapper approach: canopy-level analysis. IEEE Trans Geosci Remote Sens 48(2):4133–4142

Conese C, Maselli F (1992) Use of error matrices to improve area estimates with maximum likelihood classification procedures. Remote Sens Environ 40:113–124

Coops NC, White JD, Scott NA (2004) Estimating fragmentation effects on simulated forest net primary productivity derived from satellite imagery. Int J Remote Sens 25: 819–838

Curran PJ (1989) Remote sensing of foliar chemistry. Remote Sens Environ 30(3):271–278

Curran PJ (2001) Imaging spectrometry for ecological applications. JAG 3:305–312

Curran PJ, Dungan JL, Peterson DL (2001) Estimating the foliar biochemical concentration of leaves with reflectance spectrometry: testing the Kokaly and Clark methodologies. Remote Sens Environ 76:349–359

Dash J, Curran PJ (2007) Evaluation of the MERIS terrestrial chlorophyll index (MTCI). Adv Space Res 39:100–104

Datt B (1998) Remote sensing of chlorophyll *a*, chlorophyll *b*, chlorophyll *a* & *b* and total carotenoid content in *Eucalyptus* leaves. Remote Sens Environ 66:111–121

Datt B (1999) Visible/near infrared reflectance and chlorophyll content in *Eucalyptus* leaves. Int J Remote Sens 20: 2741–2759

Davidson EA, Reis de Carvalho CJ, Vieira ICG, Figueiredo R, Moutinho P, Ishida FY, Primo dos Santos MT, Guerrero JB, Kalif K, Sabá RT (2004) Nitrogen and phosphorus limitation of biomass growth in a tropical secondary forest. Ecol Appl 14:150–163

DeFries RS, Houghton RA, Hansen MC, Field CB, Skole D, Townshend J (2002) Carbon emissions from tropical deforestation and regrowth based on satellite observations for the 1980s and 1990s. Proc Natl Acad Sci USA 99: 14256–14261

Duguay S, Eigenbrod F, Fahrig L (2007) Effects of surrounding urbanization on non-native flora in small forest patches. Landscape Ecol 22:589–599

Fearnside PM, Laurance WF (2004) Tropical deforestation and greenhouse-gas emissions. Ecol Appl 14:982–986

Garrigues S, Allard D, Baret F, Weiss M (2006) Quantifying spatial heterogeneity at the landscape scale using variogram models. Remote Sens Environ 103:81–96

Gibbs JP (1998) Distribution of woodland amphibians along a forest fragmentation gradient. Landscape Ecol 13(4): 263–268

Gibbs HK, Brown S, Niles JO, Foley JA (2007) Monitoring and estimating tropical forest carbon stocks: making REDD a reality. Environ Res Lett 2:1–13

Giertz S, Junge B, Diekkrüger B (2005) Assessing the effects of land use change on soil physical properties and hydrological processes in the sub-humid tropical environment of West Africa. Phys Chem Earth Parts A/B/C 30:485–496

Gitelson AA, Merzlyak MN (1997) Remote estimation of chlorophyll content in higher plant leaves. Int J Remote Sens 18:2691–2697

Greenland DJ, Kowal JML (1960) Nutrient content of the moist tropical forest of Ghana. Plant Soil 12:154–173

Groffman PM, Turner CL (1995) Plant productivity and nitrogen gas fluxes in a tallgrass prairie landscape. Landscape Ecol 10(5):255–266

Groom G, Mücher C, Ihse M, Wrbka T (2006) Remote sensing in landscape ecology: experiences and perspectives in a European context. Landscape Ecol 21:391–408

Herrera J, García D, Morales J (2011) Matrix effects on plant-frugivore and plant-predator interactions in forest fragments. Landscape Ecol 26:125–135

Horler DNH, Dockray M, Barber J (1983) The red edge of plant leaf reflectance. Int J Remote Sens 4:273–288

Huang W, Wang J, Wang Z, Zhaochun J, Wang J (2004) Inversion of foliar biochemical parameters at various physiological stages and grain quality indicators of winter wheat with canopy reflectance. Int J Remote Sens 25:2409–2419

Iverson LR, Graham RL, Cook EA (1989) Applications of satellite remote sensing to forested ecosystems. Landscape Ecol 3:131–143

Jupp DLB, Strahler AH, Woodcock CE (1988) Autocorrelation and regularisation in digital images. I. Basic theory. IEEE Trans Geosci Remote Sens 26:463–473

Kokaly RF, Clark RN (1999) Spectroscopic determination of leaf biochemistry using band-depth analysis of absorption features and stepwise multiple linear regression. Remote Sens Environ 67:267–287

Lauga J, Joachim J (1992) Modelling the effects of forest fragmentation on certain species of forest-breeding birds. Landscape Ecol 6:183–193

Leakey RRB, Simons AJ (1998) The domestication and commercialization of indigenous trees in agroforestry for the alleviation of poverty. Agrofor Syst 38:165–176

Lizée M-H, Manel S, Mauffrey J-F, Tatoni T, Deschamps-Cottin M (2012) Matrix configuration and patch isolation influences override the species-area relationship for urban butterfly communities. Landsc Ecol 27:159–169

Malhi Y, Grace J (2000) Tropical forests and atmospheric carbon dioxide. Trends Ecol Evol 15:332–337

Matson P, Johnson L, Billow C, Miller J, Pu R (1994) Seasonal patterns and remote spectral estimation of canopy chemistry across the Oregon transect. Ecol Appl 4:280–298

May FE, Ash JE (1990) An assessment of the allelopathic potential of *Eucalyptus*. Aust J Bot 38:245–254

McDonald MA, Healey JR, Stevens PA (2002) The effects of secondary forest clearance and subsequent land-use on erosion losses and soil properties in the Blue Mountains of Jamaica. Agric Ecosyst Environ 92:1–19

McGarigal K, Cushman S, Stafford S (2000) Multivariate statistics for wildlife and ecology research. Springer, New York

Mooney HA (ed) (1986) Photosynthesis plant ecology. Blackwell Scientific, Oxford

Murwira A, Skidmore AK (2006) Monitoring change in the spatial heterogeneity of vegetation cover in an African savannah. Int J Remote Sens 27:2255–2269

Mutanga O, Skidmore AK, Prins HHT (2004) Predicting in situ pasture quality in the Kruger National Park, South Africa, using continuum-removed absorption features. Remote Sens Environ 89:396–408

Mutanga O, Adam E, Cho MA (2012) High density biomass estimation for wetland vegetation using WorldView-2 imagery and random forest regression algorithm. Int J Appl Earth Obs Geoinf 18:399–406

Ndlovu N, Luck-Vogel M, Schloms B, Cho M (2011) The quantification of human impact on the Dukuduku indigenous forest from 1960 to 2008 using GIS techniques as a basis for sustainable management. Fifth natural forest and wood land symposium Richard Bay KwaZulu Natal, Department of Agriculture Forestry and Fisheries South Africa, Richard bay South Africa

Novozamsky I, Houba VJK, Van Eck R, Van Vark W (1983) A novel digestion technique for multi-element plant analysis. Commun Soil Sci Plant Anal 14:239–249

Nye PH (1960) Organic matter and nutrient cycles under moist tropical forest. Plant Soil 13:333–346

Olofsson P, Foody GM, Stehman SV, Woodcock CE (2013) Making better use of accuracy data in land change studies: estimating accuracy and area and quantifying uncertainty using stratified estimation. Remote Sens Environ 129: 122–131

Ozdemir I, Karnieli A (2011) Predicting forest structural parameters using the image texture derived from WorldView-2 multispectral imagery in a dryland forest, Israel. Int J Appl Earth Obs Geoinf 13(5):701–710

Piccolo MC, Neill C, Cerri CC (1994) Net nitrogen mineralization and net nitrification along a tropical forest-to-pasture chronosequence. Plant Soil 162:61–70

Prasad A (2003) Book review, Lessons from Amazonia, The Ecology and Conservation of a Fragmented Forest. Landsc Ecol 18:214–215

Ramoelo A, Skidmore AK, Cho MA, Schlerf M, Mathieu R, Heitkönig IMA (2012) Regional estimation of savanna grass nitrogen using the red-edge band of the spaceborne RapidEye sensor. Int J Appl Earth Obs Geoinf 19:151–162

Richter R, Schlapfer D (2002) Geo-atmospheric processing of airborne imaging spectrometry data. Part 2. Atmospheric/topographic correction. Int J Remote Sens 23:2631–2649

Rouse JW, Haas RH, Schell JA, Deering DW, Harlan JC (1974) Monitoring the vernal advancement and retrogradation of natural vegetation NASA/GSFC Type III Final Report. Greenbelt, p 371

Saunders DA, Hobbs RJ, Margules CR (1991) Biological consequences of ecosystem fragmentation: a review. Conserv Biol 5:18–32

Simons AJ, Leakey RRB (2004) Tree domestication in tropical agroforestry. Agrofor Syst 61:167–181

Skidmore A (1999) Accuracy assessment of spatial information. In: Stein A, van der Meer F, Gorte B (eds) Spatial statistics for remote sensing. Kluwer Academic Publishers, Dordrecht, pp 197–209

Smith M-L, Ollinger SV, Martin ME, Aber JD, Hallett RA, Goodale CL (2002) Direct estimation of aboveground forest productivity through hyperspectral remote sensing of canopy nitrogen. Ecol Appl 12:1286–1302

Van der Werf GR, Morton DC, DeFries RS, Olivier JGJ, Kasibhatla PS, Jackson RB, Collatz GJ, Randerson JT (2009) CO_2 emissions from forest loss. Nat Geosci 2:737–738

Van Heerden IL 2011 Management concepts for the Mfolozi flats and estuary as a component of the management of the iSimangaliso Wetland Park. In: Bate GC, Whitfield AK, Forbes AT (eds) 2011 A review of studies on the Mfolozi estuary and associated flood plain with emphasis on information required by management for future reconnection of the river to the St. Lucia system Report to the Water Research Commission WRC Report No. KV 255/10. Pretoria: WRC

Van Wyk GF, Everard DA, Midgley JJ, Gordon IG (1996) Classification and dynamics of a southern African subtropical coastal lowland forest. S Afr J Bot 62:133–142

Vasconcelos HL, Luizão FJ (2004) Litter production and litter nutrient concentrations in a fragmented amazonian landscape. Ecol Appl 14:884–892

Vitousek P (1982) Nutrient cycling and nutrient use efficiency. Am Nat 119:553–572

Vitousek PM, Sanford RL Jr (1986) Nutrient cycling in moist tropical forest. Annu Rev Ecol Syst 17:137–167

Yoder BJ, Pettigrew-Crosby RE (1995) Predicting nitrogen and chlorophyll content and concentrations from reflectance spectra (400–2500 nm) at leaf and canopy scales. Remote Sens Environ 53:199–211

Zengeya FM, Mutanga O, Murwira A (2013) Linking remotely sensed forage quality estimates from WorldView-2 multispectral data with cattle distribution in a savanna landscape. Int J Appl Earth Obs Geoinf 21:513–524